Inorg. Chem. **2008**, *47*, 7948−7950

Inorganic Chemistry
Communication

Mixed-Valence $Cu^{II}Cu^{I}_{15}I_{17}$ Cluster Builds up a 3D Metal−Organic Framework with Paramagnetic and Thermochromic Characteristics

Jun He,[†,‡] Jing-Xiang Zhang,[†] Chun-Kwan Tsang,[‡] Zhengtao Xu,[*,‡] Ye-Gao Yin,[*,†] Dan Li,[†] and Seik-Weng Ng[§]

Department of Chemistry, Shantou University, Guangdong 515063, China, Department of Biology and Chemistry, City University of Hong Kong, 83 Tat Chee Avenue, Kowloon, Hong Kong, China, and Department of Chemistry, University of Malaya, Kuala Lumpur 50603, Malaysia

Received May 20, 2008

Four cubane-like Cu_4I_4 units are assembled around an iodine atom to form the giant, mixed-valent $Cu^{II}Cu^{I}_{15}I_{17}$ cluster. The $Cu^{II}Cu^{I}_{15}I_{17}$ cluster and a bipyrazole linker form a 3D open framework with paramagnetic and thermochromic properties. This paper also touches on the resemblance of this cluster to the self-similar object of a Sierpinski tetrahedron.

One prominent trend in the field of metal−organic frameworks (MOFs) is to use secondary building units (SBUs) with rigid and regular geometry for interlinking of the organic molecules, in order to achieve advanced structural features as well as solid-state properties. Compared with the single metal ion, the SBU consists of several metal centers and the associated donor species, serving to enlarge the metric scale of the solid-state network and to enrich the structural and functional possibilities. For instance, SBUs of metal carboxylate clusters have been widely used to direct and effect the construction of highly symmetrical 3D frameworks with diverse topological and porous characteristics.[1,2]

In contrast to the generally weak electroactivity of the metal carboxylate systems, cluster units of the more polarizable chalcogenides[3−5] and halides[6,7] tend to impart richer electronic features to the resultant networks. Among the numerous MOFs involving chalcogenide or halide clusters, the ones with 3D open-framework features are especially notable[5,6] because of the aesthetic appeal as well as the possibility of combining porosity and enhanced electronic properties in these systems. Overall, it remains of great interest to uncover electronically active cluster systems that can be effectively integrated into crystalline MOFs.

As part of our effort to achieve electroactive MOFs, we here report a 3D framework based on a large, mixed-valent $Cu^{II}Cu^{I}_{15}I_{17}$ cluster and the ligand $tmbpzH_2$,[8] 3,3′,5,5′-tetramethyl-4,4′-bipyrazole [$Cu^{II}Cu^{I}_{15}I_{17}(tmbpzH_2)_6$, henceforth called **1**]. Compound **1** features a simple cubic net (i.e., the α-Po net) that topologically parallels the prototypical sodalite and zinc(II) carboxylate MOF-5,[1a] while displaying marked differences in both the local bonding motifs and crystallographic acentricity. Among the reported discrete Cu−I cluster SBUs of coordination networks,[5d,9] the

---

* To whom correspondence should be addressed. E-mail: zhengtao@cityu.edu.hk (Z.X.), ygyin@stu.edu.cn (Y.-G.Y.).

[†] Shantou University.

[‡] City University of Hong Kong.

[§] University of Malaya.

(1) (a) Li, H.; Eddaoudi, M.; O'Keeffe, M.; Yaghi, O. M. *Nature* **1999**, *402*, 276–279. (b) Chen, B. L.; Eddaoudi, M.; Hyde, S. T.; O'Keeffe, M.; Yaghi, O. M. *Science* **2001**, *291*, 1021–1023. (c) Chae, H. K.; Siberio-Perez, D. Y.; Kim, J.; Go, Y. B.; Eddaoudi, M.; Matzger, A. J.; O'Keeffe, M.; Yaghi, O. M. *Nature* **2004**, *427*, 523–527. (d) Sudik, A. C.; Millward, A. R.; Ockwig, N. W.; Cote, A. P.; Kim, J.; Yaghi, O. M. *J. Am. Chem. Soc.* **2005**, *127*, 7110–7118.

(2) (a) Wang, X.-S.; Ma, S.; Sun, D.; Parkin, S.; Zhou, H.-C. *J. Am. Chem. Soc.* **2006**, *128*, 16474–16475. (b) Ma, S.; Sun, D.; Ambrogio, M.; Fillinger, J. A.; Parkin, S.; Zhou, H.-C. *J. Am. Chem. Soc.* **2007**, *129*, 1858–1859. (c) Sun, D.; Ke, Y.; Collins, D. J.; Lorigan, G. A.; Zhou, H.-C. *Inorg. Chem.* **2007**, *46*, 2725–2734.

(3) (a) Zheng, N.; Bu, X.; Lauda, J.; Feng, P. *Chem. Mater.* **2006**, *18*, 4307–4311. (b) Zheng, N.; Bu, X.; Lu, H.; Chen, L.; Feng, P. *J. Am. Chem. Soc.* **2005**, *127*, 14990–14991. (c) Yuan, M.; Dirmyer, M.; Badding, J.; Sen, A.; Dahlberg, M.; Schiffer, P. *Inorg. Chem.* **2007**, *46*, 7238–7240.

(4) (a) Song, L.; Li, J.; Lin, P.; Li, Z.; Li, T.; Du, S.; Wu, X. *Inorg. Chem.* **2006**, *45*, 10155–10161. (b) Selby, H. D.; Orto, P.; Zheng, Z. *Polyhedron* **2003**, *22*, 2999–3008. (c) Liang, K.; Zheng, H.-G.; Li, Y.-Z.; Xin, X.-Q. *Inorg. Chem. Commun.* **2007**, *10*, 1164–1167.

(5) (a) Lang, J.-P.; Xu, Q.-F.; Yuan, R.-X.; Abrahams, B. F. *Angew. Chem., Int. Ed.* **2004**, *43*, 4741–4745. (b) Jin, S.; DiSalvo, F. J. *Chem. Mater.* **2002**, *14*, 3448–3457. (c) Liang, K.; Zheng, H.; Song, Y.; Lappert, M. E.; Li, Y.; Xin, X.; Huang, Z.; Chen, J.; Lu, S. *Angew. Chem., Int. Ed.* **2004**, *43*, 5776–5779. (d) Wang, X.-L.; Qin, C.; Wang, E.-B.; Su, Z.-M.; Li, Y.-G.; Xu, L. *Angew. Chem., Int. Ed.* **2006**, *45*, 7411–7414.

(6) (a) Zhang, J.; Lachgar, A. *J. Am. Chem. Soc.* **2007**, *129*, 250–251. (b) Bennett, M. V.; Beauvais, L. G.; Shores, M. P.; Long, J. R. *J. Am. Chem. Soc.* **2001**, *123*, 8022–8032.

(7) (a) Zhou, H.; Lachgar, A. *Eur. J. Inorg. Chem.* **2007**, 1053–1066. (b) Beauvais, L. G.; Long, J. R. *Inorg. Chem.* **2006**, *45*, 236–243.

(8) (a) He, J.; Yin, Y.; Wu, T.; Li, D.; Huang, X. *Chem. Commun.* **2006**, 2845–2847. (b) Zhang, J.-P.; Kitagawa, S. *J. Am. Chem. Soc.* **2008**, *130*, 907–917. (c) Zhang, J.-P.; Horike, S.; Kitagawa, S. *Angew. Chem., Int. Ed.* **2007**, *46*, 889–892.

(9) (a) Xue, X.; Wang, X.-S.; Xiong, R.-G.; You, X.-Z.; Abrahams, B. F.; Che, C.-M.; Ju, H.-X. *Angew. Chem., Int. Ed.* **2002**, *41*, 2944–2946. (b) Hu, S.; Tong, M.-L. *Dalton Trans.* **2005**, 1165–1167. (c) Wang, J.; Zheng, S.-L.; Hu, S.; Zhang, Y.-H.; Tong, M.-L. *Inorg. Chem.* **2007**, *46*, 795–800. (d) Bi, M.; Li, G.; Zou, Y.; Shi, Z.; Feng, S. *Inorg. Chem.* **2007**, *46*, 604–606.

10.1021/ic8009207 CCC: $40.75

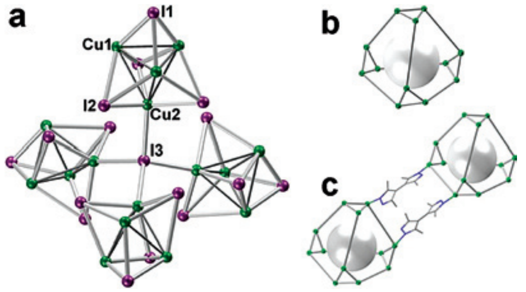

Figure 1. (a) Tetrahedral building unit of $Cu^{II}Cu^{I}_{15}I_{17}$ in **1**, consisting of one iodine atom at the center and one Cu_4I_4 subunit at each corner; Cu···Cu interactions are shown as dark gray bonds, and the crystallographically independent copper and iodine atoms are labeled. (b) Simplified picture of part a: the longer links between the Cu1 atoms along the tetrahedral edges highlight the tetrahedral shape and do not indicate chemical interaction. A large gray sphere is placed inside to enhance the 3D effect. (c) Two neighboring truncated tetrahedra linked by two $tmbpzH_2$ ligands.

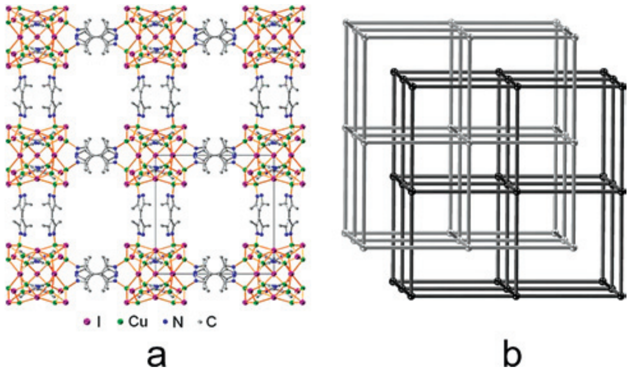

Figure 2. (a) Single net of $Cu^{II}Cu^{I}_{15}I_{17}$ clusters and $tmbpzH_2$ molecules in **1** (Cu−N distance: 2.016 Å). (b) Topological representation of **1** showing the 2-fold interpenetration (sphere: center of the cluster).

$Cu^{II}Cu^{I}_{15}I_{17}$ cluster in **1** is quite unique in its mixed-valent state and its giant size. Generally, MOFs with integrated mixed-valent features remain relatively undeveloped, even though mixed-valent tin and gold halides templated with organic ammonium cations have been achieved.[10] In the present system, the $Cu^{II}Cu^{I}_{15}I_{17}$ cluster gives rise to distinct fluorescent emission and thermochroism, and the mixed-valent feature generates paramagnetic behavior in the solid-state network. In spite of the serendipitous nature of its discovery, the above features of **1** serve to highlight the rich potential of halide cluster building blocks in tackling the topical issue of combining open-framework features and accentuated electronic properties.

Crystals of **1** were obtained in a solvothermal reaction of equimolar amounts of $tmbpzH_2$, CuSCN, and excess KI in water at 140 °C (see the Supporting Information). **1** crystallizes in the acentric space group $P\bar{4}3n$ (No. 218),[11] featuring three types of crystallographically independent iodine sites (I1, I2, and I3, with respective site occupancy factors $^1/_3$, 1 and $^1/_{12}$), two types of copper sites (Cu1 and Cu2, with respective site occupancy factors 1 and $^1/_3$), and half of the $tmbpzH_2$ moieties. The $Cu^{II}Cu^{I}_{15}I_{17}$ cluster belongs to the rare *T* point group (Figure 1a), with an iodine atom (I3) at the center of the tetrahedron and a Cu_4I_4 cubane-like subunit at every vertex (the Cu_4I_4 subunits are related by the C_2 axes bisecting the C_3 axes; there is no reflection symmetry for the overall cluster). The central iodine atom bonds to one of the copper atoms (Cu2) of the Cu_4I_4 subunit with a Cu−I distance of 2.744 Å. The other three copper atoms (Cu1) in the Cu_4I_4 subunit are related by the C_3 element, and they form an equilateral triangle with a Cu···Cu interaction of 2.710 Å. With its C_3 axis coinciding with that of the overall $Cu^{II}Cu^{I}_{15}I_{17}$ cluster, the Cu1 triangle approaches the Cu2 atom, forming a slightly elongated Cu_4 tetrahedron, with a longer Cu1···Cu2 distance at 2.892 Å. Each of the four faces of the Cu_4 tetrahedron is then capped by an iodine atom to complete the distorted cubane of the Cu_4I_4 subunit. The rotational and reflection symmetries of the Cu4 tetrahedron are preserved in the Cu_4I_4 subunit, with the Cu1 equilateral triangle capped by the I1 atom (Cu1−I1 distance: 2.588 Å) and the three isosceles triangles by the crystallographically equivalent I2 atoms (distances: Cu1−I2, 2.849 Å; Cu2−I2, 2.615 Å). The symmetry of the $Cu^{II}Cu^{I}_{15}I_{17}$ cluster indicates that the Cu^{2+} site is either delocalized at the X-ray crystallography time scale or localized but crystallographically disordered.

The tetrahedrally shaped $Cu^{II}Cu^{I}_{15}I_{17}$ clusters are interlinked by the linear $tmbpzH_2$ ligands into a 3D open framework that can be topologically represented as the primitive cubic net (i.e., the α-Po net; Figure 2a), with each rod of the net involving two bridging $tmbpzH_2$ ligands and each node standing for the $Cu^{II}Cu^{I}_{15}I_{17}$ cluster. The crystal structure consists of two interpenetrated cubic nets thus formed (Figure 2b) but remains noncentrosymmetric ($P\bar{4}3n$), with the two homochiral interpenetrated nets being related by the translational vector ($^1/_2$, $^1/_2$, $^1/_2$).

Complexes of the Cu_4I_4 cluster often display two distinct emission bands with temperature-dependent relative intensities (i.e., luminescent thermochromism).[9b,d,12] As seen in Figures S1 and S2 in the Supporting Information, the emission maximum of **1** occurs at 482 nm at 10 K and continuously red shifts to 542 nm at 300 K with increasing temperature, which is consistent with the intensity evolution observed of $Cu_4I_4py_4$; i.e., the high-energy emission dominates at low temperature, and the low-energy band intensifies at high temperature. However, the tapering features of the emission peaks (beyond 700 nm), as well as the significantly blue-shifted low-energy emission, point to substantial differences of the electronic structures between **1** and the Cu_4I_4 complexes.

The mixed-valence character of **1** is supported by the magnetic property measurements, in spite of the relatively weak paramagnetism due to the diluted copper(II) character. Notice that, with only one copper(II) center for every unit

---

(10) (a) Castro-Castro, L. M.; Guloy, A. M. *Angew. Chem., Int. Ed.* **2003**, *42*, 2771–2774. (b) Castro-Castro, L. M.; Guloy, A. M. *Inorg. Chem.* **2004**, *43*, 4537–4539. (c) Guan, J.; Tang, Z.; Guloy, A. M. *Chem. Commun.* **2005**, 48–50.

(11) Crystal data for **1**: $C_{60}H_{84}Cu_{16}I_{17}N_{24}$, cubic, space group $P\bar{4}3n$ (No. 218), $M_r = 4315.45$, $a = 17.3240(8)$ Å, $V = 5199.3(2)$ Å^3, $Z = 2$, $\rho_{calcd} = 2.757$ g/cm^3, $F(000) = 3954$, $T = 295(2)$ K, $\mu = 8.290$ mm^{-1}, 55 028 reflections measured, 1965 unique ($R_{int} = 0.0456$), final R1 = 0.0536, wR2 = 0.1604, $S = 1.174$ for all data.

(12) (a) Ford, P. C.; Cariati, E.; Bourassa, J. *Chem. Rev.* **1999**, *99*, 3625–3647. (b) De Angelis, F.; Fantacci, S.; Sgamellotti, A.; Cariati, E.; Ugo, R.; Ford, P. C. *Inorg. Chem.* **2006**, *45*, 10576–10584.

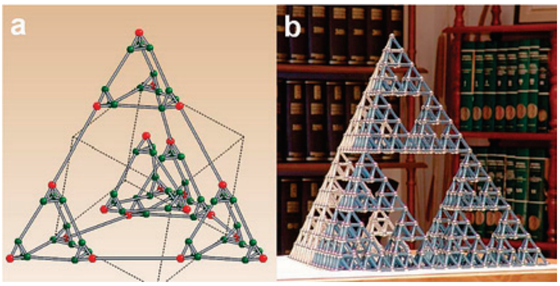

Figure 3. (a) Sierpinski tetrahedral motif in the unit cell of **1**, consisting of one $Cu_{16}I_{17}$ cluster at the body center and four at the vertices. Only the Cu1 (green) and I1 (red) atoms are shown. The longer Cu−Cu and I−I links along the tetrahedral edges outline the tetrahedral shape and do not signify chemical interaction. (b) Sierpinski tetrahedron model with a fractal order of 5. Reprinted with permission from http://textodigital.com. Copyright 2006−2008 Rafael Millán.

of $Cu_{16}I_{17}(C_{10}H_{14}N_4)_6$ (formula weight: 4315), the molar paramagnetic susceptibility, expected to be about 1.25×10^{-3} cm^3 mol^{-1} at room temperature, is already rivaled by the molar diamagnetic susceptibility (-1.603×10^{-3} cm^3 mol^{-1}, calculated from the Pascal constants). After correction for diamagnetism, paramagnetic susceptibility (χ_M) data for **1** were obtained from 300 to 2 K at an applied field of 1000 Oe (Figure S3a in the Supporting Information). At 300 K, $\chi_M T = 0.39$ cm^3 K mol^{-1} is in apparent accordance with one unpaired electron (0.375 cm^3 K mol^{-1} for $S = {}^1/_2$) in each cluster unit of $Cu^{II}Cu^{I}_{15}I_{17}$. The value of $\chi_M T$ decreases in an almost linear fashion and reaches 0.01 cm^3 K mol^{-1} at 2 K, which, in a superficial fitting of the Curie−Weiss formulation, would suggest strong antiferromagnetic interaction. However, the large separation provided by the molecule $tmbpzH_2$ should obviate significant coupling across the $Cu_{16}I_{17}$ clusters, and therefore factors other than antiferromagnetic coupling across the $tmbpzH_2$ molecules should be invoked to account for the temperature dependence of $\chi_M T$. Interestingly, the plot of $1/\chi_M$ versus temperature features a steep descent below 50 K, indicating an attendant sharp decrease of the Curie constant C (and thus the effective magnetic moment μ_{eff}). The underlying change in the electronic states populated by the unpaired electron is apparently profound, and further studies are needed to elucidate the magnetic behavior in this mixed-valence system. Additionally, the deconvoluted X-ray photoelectron spectroscopy (XPS) spectrum consists of two peaks in an approximate ratio of 1:15, with the weaker peak at higher energy, consistent with the $Cu^{I}_{15}Cu^{II}$ assignment (Figure S5 in the Supporting Information). **1** is electron spin resonance silent at room temperature.

We now comment on the distinct self-similar motif of the tetrahedral geometry within the unit cell of **1**. For visualization, let us focus on the distribution of the individual $Cu_{16}I_{17}$ clusters (to highlight the tetrahedral shape, only the I1 and Cu1 atoms are shown in Figure 3a). The clusters are located at the vertices and the body center of the unit cell, and they are related by translation symmetry and oriented in the same direction. Of these, the eight clusters at the vertices belong to the same coordination net, whereas the one at the center belongs to the other net.

Featured in Figure 3a are four of the vertex-occupying clusters that, in turn, form a larger tetrahedron. Notice that the vertices and edges of this larger tetrahedron coincide with those of the constituent clusters. On the level of the individual $Cu_{16}I_{17}$ cluster, one finds a similar geometric relationship between the overall cluster and the smaller tetrahedra formed by the I1 and Cu1 atoms at the corners. The self-similar features thus extracted resemble the famous Sierpinski tetrahedron (Figure 3b), which, in the second order of fractal, is obtained by cutting a tetrahedron at the midpoints of the edges to make four smaller tetrahedra (the octahedral volume at the center is hollowed out). One repeats the same process on the resultant tetrahedra to generate the third order of fractal, and so on. In this regard, the overall tetrahedral structure (without the cluster at the center) in Figure 3a has an order of fractal of 3, while the one in Figure 3b has an order of 5.

In a broad sense, an infinite and periodic lattice invariably imbeds self-similar features; for example, in a square net, the primitive square cell is surrounded by six contiguous peers that, in turn, form a larger square cell. By comparison, the formation of self-similarity not directly resulting from translation symmetry (e.g., within a unit cell or a discrete chemical entity) appears to be a more meaningful exercise, as is reflected in dendrimers and other fractal constructs.[13] As another example, the widely publicized supertetrahedral chalcogenide clusters[14] also feature the Sierpinski tetrahedral motif. The concept of self-similarity is ubiquitous,[15] and shall find even more use in structural chemistry.

Acknowledgment. We thank Wei-Xiong Zhang for help with magnetic property studies. This work is supported by RGC of HKSAR [Project 9041109 (CityU 102406)].

Supporting Information Available: Crystallographic data in CIF format, experimental details, luminescence spectra, magnetization plots, powder X-ray diffraction patterns, XPS spectra, and thermogravimetric analysis/differential thermal analysis plots for **1**. This material is available free of charge via the Internet at http://pubs.acs.org.

IC8009207

---

(13) (a) Newkome, G. R.; Wang, P.; Moorefield, C. N.; Cho, T. J.; Mohapatra, P. P.; Li, S.; Hwang, S.-H.; Lukoyanova, O.; Echegoyen, L.; Palagallo, J. A.; Iancu, V.; Hla, S.-W. *Science* **2006**, *312*, 1782–1785. (b) Newkome, G. R.; Moorefield, C. N.; Vötle, F. *Dendrimers and Dendrons: Concepts, Syntheses, Applications*; Wiley-VCH: Weinheim, Germany, 2001. (c) Sugiura, K.-I.; Tanaka, H.; Matsumoto, T.; Kawai, T.; Sakata, Y. *Chem. Lett.* **1999**, 1193–1194. (d) Teo, B.; Zhang, H. *Proc. Natl. Acad. Sci. U.S.A.* **1991**, *88*, 5067–5071.

(14) Feng, P.; Bu, X.; Zheng, N. *Acc. Chem. Res.* **2005**, *38*, 293–303.

(15) Mandelbrot, B. B. *The Fractal Geometry of Nature*; Freeman: San Francisco, CA, 1982.